10. Summary and Application Example

This document records in detail an effort to assess current nonlinear static procedures (NSPs) given in FEMA 356 and ATC-40 for the seismic analysis and evaluation of structures. In addition, the document presents approaches that were developed to improve these procedures for future application by practicing engineers. Not all of the portions of the two documents were evaluated. Conclusions regarding the relative accuracy or technical soundness of these documents should not be inferred beyond the specific material and discussions contained in this document.

The purpose of this summary is to present a practical overview of the results and to illustrate the application of NSPs, that include the proposed improvements for an example building. Sections 10.1 through 10.8 contain key results of analytical studies conducted as part of this project and resulting suggestions for specific changes to existing procedures for nonlinear static analysis procedures. Section 10.9 discusses some important aspects of uncertainty and reliability of nonlinear static procedures and the suggestions for improvement. Section 10.10 summarizes some key observations with respect to shortcomings of inelastic seismic analysis procedures that were not fully resolved in this project. These are areas in which significant improvement might be made in the future. Section 10.11 is the application example.

10.1 Overview of Inelastic Seismic Analysis Procedures

Nonlinear static procedures are one type of inelastic analysis that can be used to estimate the response of structures to seismic ground shaking. The differences among the various approaches to inelastic analysis in general relate to the level of detail of the structural model and the characterization of the seismic ground shaking. Detailed structural models can often be simplified into equivalent multi-degree-of-freedom models; or, in some cases, single-degree-of-freedom oscillator models, as with nonlinear static procedures. The most detailed characterizations of seismic ground motion are actual ground motion records that comprise accelerations, velocities, and displacements expected at the ground surface at a specific site. A simplification can be made by representing the effects ground motion has in the frequency domain with response spectra that plot maximum response of an elastic SDOF oscillator as a function of period. This is the type of characterization normally used for nonlinear static procedures.

The discussion in Chapter 2 includes basic descriptions of the two nonlinear static procedures that are currently used in practice. FEMA 356 uses a displacement modification procedure (Coefficient Method) in which several empirically derived factors are used to modify the response of a single-degree-of-freedom model of the structure, assuming that it remains elastic. The alternative Capacity-Spectrum Method of ATC-40 is actually a form of equivalent linearization. This technique uses empirically derived relationships for the effective period and damping as a function of ductility to estimate the response of an equivalent linear SDOF oscillator.

10.2 Evaluation of Current Nonlinear Static Procedures

In practice, the current procedures can result in estimates of maximum displacement that are significantly different from one another. This has caused concern on the part of practicing engineers. One of the major objectives of the project was to ascertain the reasons for these differences and to try to correct both procedures to produce similar results. Chapter 3 documents a comprehensive evaluation of both procedures. The basic technique was to develop a series of nonlinear single-degree-of-freedom oscillators of varying period, strength, and hysteretic behavior. These were subjected to ground motion representing different site soil conditions. The resulting database of approximately 180,000 predictions of maximum displacement was used as a benchmark to judge the accuracy of the approximate NSPs. This was accomplished by comparing the estimates for each oscillator from both NSPs to the results of the nonlinear response-history analyses. Differences in the two estimates were compiled and compared in a statistical study.

10.2.1 Key Observations: ATC-40 Version of Capacity-Spectrum Method

Longer-period response. The ATC-40 procedures for structures with hysteretic behavior type A tended to underestimate the maximum displacement response for inelastic systems. The underestimation averages 25% to 35% for systems with periods longer than about 0.7 s.

For structures with hysteretic behavior type B, the ATC-40 procedures led to small underestimations or small overestimations of lateral displacement of systems with periods longer than about 0.6 s. Whether

ATC-40 underestimates or overestimates depends on the level of lateral strength and on the site class.

For structures with hysteretic behavior type C, the ATC-40 procedures led to overestimations of the maximum displacement for all periods. The overestimation increases as R increases. Average overestimations for periods greater than 0.5 s range from approximately 5% for systems with $R = 1.5$ to about 35% for systems with $R = 8$.

Shorter-period response. The ATC-40 procedures can lead to significant overestimations of the maximum displacements of inelastic oscillators for periods shorter than those noted above. The overestimations increase with decreasing strength. Estimated displacements in the short-period range can be, on average, up to two times larger than the benchmark displacements from response-history analyses.

Degrading stiffness and strength. ATC-40 assumes that the inelastic deformation demands in structures with behavior type B will be larger than those in structures with behavior type A, while results of nonlinear response-history analyses show that the deformations are actually approximately the same or slightly larger for the elastic-perfectly-plastic (EPP) model as compared to the stiffness-degrading (SD) model. The current provisions of ATC-40 do not address the potential dynamic instability that can arise in systems with in-cycle strength degradation and/or P-delta effects.

Limitations on damping and spectral reduction factors. ATC-40 specifies limits on effective damping that result in the imposition of minimum spectral-reduction factors based on the anticipated performance of building types. These limitations were based on engineering judgment that has not been borne out in the analytical studies reported here. While the intention of these limitations may have been to provide some conservatism for degrading structures, the resulting estimates of displacement exceed expected mean values when compared with actual behavior for many cases.

10.2.2 Key Observations: FEMA 356 and the Coefficient Method

Transition period for the equal-displacement approximation. Nonlinear dynamic analyses demonstrate that the total displacement experienced by long-period structures that undergo inelastic response tends to be about the same as structures of the same period, responding in an elastic manner, leading to the so-called equal displacement approximation. Short-period structures do not behave in this manner. FEMA-356 defines a characteristic site period to differentiate between these two types of behavior. Characteristic site periods of FEMA 356 are based on the period at the intersection of the constant-acceleration spectral region and the constant-velocity spectral region. These characteristic periods are shorter than the transition periods observed from nonlinear response-history analyses. This can result in underestimation of inelastic deformations for periods between the characteristic site period and periods that are approximately 1.5 times the characteristic site period.

Ratio of inelastic to elastic deformation, coefficient C_1. The use of the equal displacement approximation to compute the coefficient C_1 for systems with periods longer than the characteristic periods leads to relatively good approximations of maximum inelastic deformations for systems with EPP behavior for periods longer than about 1 s. Only small overestimations in the order of 5% or 10% are produced with this approximation. Note that for very soft soil sites and near-fault records, this is only true for systems with periods of vibration that are approximately 1.5 times longer than the predominant period and the pulse periods, respectively.

For systems with R larger than about 2.5, the limiting values (capping) of C_1 imposed by Section 3.3.1.3.1. of the LSP of FEMA 356 will control the estimate of maximum inelastic deformation. This can lead to theoretically large underestimates of displacements in short-period structures, particularly on soft sites.

If capping is not used, and if the transition period is lengthened, the FEMA 356 equation to calculate C_1 does not adequately capture the changes in inelastic deformation demands that are produced with changes in R for short-period structures. The magnification of inelastic displacement demands with decreasing lateral strength for short-period structures was found to be larger than that implied by FEMA 356.

Degradation of stiffness and strength (Coefficients C_2 and C_3). There is not a clear division of the intent of coefficients C_2 and C_3. This problem was documented in FEMA 357. In particular, C_2 is supposed to account for changes in lateral displacement produced by departures of the hysteretic behavior from an EPP hysteretic model (such as pinching, stiffness degradation and strength degradation.). P-Δ effects are accounted for by C_3 in the current provisions of FEMA 356. FEMA 356 does not distinguish between cyclic strength degradation and in-cycle strength degradation.

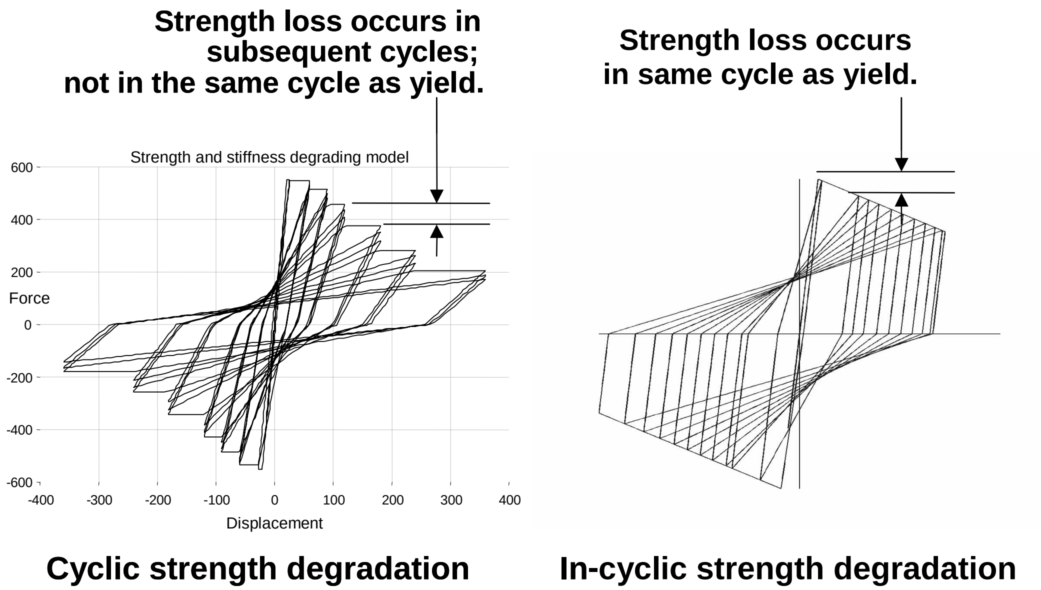

Figure 10-1 Differences between cyclic and in-cycle strength degradation

In-cycle degradation produces effects similar to *P-Δ*, which can lead to dynamic instability in weak structures.

The C_2 coefficient of FEMA 356 implies that inelastic displacement should increase for stiffness degrading systems as compared with EPP systems. With the exception of periods of vibration smaller than about 0.7 s, the maximum displacement of stiffness-degrading systems is actually very similar to or slightly smaller (5% to 10%) than the maximum displacement of EPP systems.

FEMA 356 introduced an alternative recommendation for C_2 that was not in FEMA 273, as follows: "Alternatively, use of $C_2 = 1$ shall be permitted for nonlinear procedures". The ambiguity of conflicting recommendations is confusing to users of FEMA 356.

Coefficient C_3 does not adequately address the possibility of dynamic instability.

10.3 Strength Degradation

The results of the evaluation of the NSPs suggest that both procedures would benefit from greater clarity with respect to the different types of possible degradation in structures subject to seismic shaking. This is particularly critical for degradation in strength. Chapter 4 discusses the differences between the consequences of strength loss within a single cycle of deformation (in-cycle) and that which occurs in subsequent cycles (cyclic). This important distinction illustrated in Figure 10-1. In-cycle strength degradation, including that associated with *P-Δ* effects, can lead to dynamic instability. To account for this, a lower limit on the strength of structures that exhibit strength-degrading behavior is suggested for use with nonlinear static procedures. The limit is a function of the period of the structure and the post-elastic stiffness characteristics, as modified for in-cycle strength degradation. If the structure has less strength than the limit, nonlinear dynamic analysis is recommended.

10.4 Improved Procedures for Displacement Modification

Based on the evaluation of NSPs, Chapter 5 proposes modifications to the Coefficient Method of FEMA 356. The suggestions relate primarily to the coefficients themselves. These are tabulated along with the current specifications in Table 10-1. The changes are briefly summarized as follows:

10.4.1 Summary of Findings Pertaining to Coefficient C_1

This coefficient represents the approximate ratio of the maximum displacement of an EPP SDOF oscillator model to that of a fully elastic counterpart. The proposed modification is based on the results of the simplified dynamic analyses conducted as a part of the

Table 10-1 Coefficients for Use in Equations for Effective Damping

Coefficient	*Current Specification*	*Modification*	*Purpose of Coefficient*
C_1	1.0 for $T_e \geq T_s$ $[1.0 + (R\text{-}1)T_s/T_e]/R$ for $T_e < T_s$	$C_1 = 1 + \frac{R-1}{aT^2}$ where a = 130 for site class B 90 for site class C 60 for site class D	Convert max. elastic displacement to estimate for inelastic system
C_1 (with short T "cap")	1.5 for $T_e < 0.1$s interpolating to 1.0 for $T_e \geq T_s$	Not recommended	
C_2 (degrading systems)	Immediate Occupancy 1.0 Life Safety 1.3 for $T \leq 0.1$ interpolating to 1.1 for $T \geq T_s$ Collapse Prevention 1.5 for $T \leq 0.1$ interpolating to 1.2 for $T \geq T_s$	$C_2 = 1 + \frac{1}{800}\left[\frac{R-1}{T}\right]^2$ recommended only for structures with significant stiffness and/or strength degradation	Hysteretic pinching Cyclic degradation
C_2 (non-degrading systems)	1.0	1.0	
C_3	$1.0 + \frac{\lvert\alpha\rvert(R-1)^{3/2}}{T_e}$	Eliminate in favor of strength limit	*P-Δ* In-cycle degradation

evaluation database. The proposed relationship is a function of strength (R), period (T), and site class.

The current provisions of FEMA 356 allow the C_1 coefficient to be limited for short-period structures. Although this limitation was intended to recognize that short-period buildings do not respond as often predicted by analysis, the basis of the limitation is subjective. For this reason, the use of the "cap" on C_1 is not recommended. However, the effects of soil-structure interaction can have a mitigating effect on maximum inelastic displacements of short-period structures. Some rational procedures for including the SSI effect in nonlinear static analyses are presented in Chapter 8.

10.4.2 Summary of Findings Pertaining to Coefficient C_2

This coefficient accounts for the change in maximum inelastic displacement for systems that exhibit cyclic degradation of stiffness and strength. The proposed modification is based on the results of the simplified dynamic analyses conducted as a part of the evaluation database. In many cases, the data suggest that cyclic degradation does not increase maximum displacements. However, there are exceptions, especially for short-period, low-strength structures.

10.4.3 Summary of Findings Pertaining to Coefficient C_3

This coefficient was intended to account for *P-Δ* effects. Review of related research and results of detailed analyses indicate that maximum inelastic displacements tend to increase abruptly, leading to dynamic instability and implied collapse for relatively weak structures. The point at which this transition occurs is related to the strength, period, and post-elastic stiffness of the structure. Although the current expression includes these variables, it does not predict the instability. The recommendation is for a limit on minimum strength (maximum *R*) for structural models that exhibit strength degradation. This limit eliminates the need for the C_3 coefficient.

10.5 Improved Procedures for Equivalent Linearization

Many engineers favor working with the Capacity-Spectrum Method, a form of equivalent linearization. This is likely due, at least in part, to the intuitive nature of the procedure that graphically relates "capacity" to "demand." Chapter 6 presents the results of an effort to improve the practical application of equivalent linearization procedures. The resulting suggestions focus on improved estimates of equivalent period and damping. These differ from the assumptions in ATC-40. Generally, the optimal effective period is less than the secant period (see Figure 10-2). The optimal

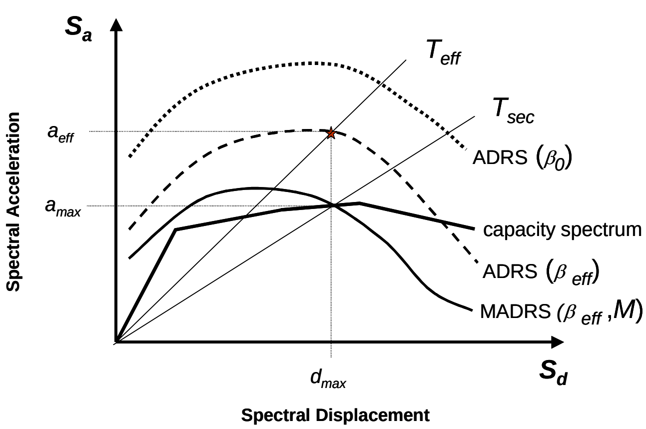

Figure 10-2 Acceleration-displacement response spectrum (ADRS) showing effective period and damping parameters of equivalent linear system, along with a capacity curve.

effective damping is also less than that specified in ATC-40. Note also in Figure 10-2 that the optimal effective period does not intersect the capacity spectrum for the structure at the maximum inelastic displacement or Performance Point. In order to preserve this useful visualization feature, Chapter 6 also includes an optional adjustment to generate a modified acceleration-displacement response spectrum (MADRS) that does intersect the capacity spectrum at the Performance Point. Similar to the current ATC-40 procedure, the effective period and damping are both dependent on ductility and consequently, an iterative or graphical technique is required to calculate the Performance Point. Several options are outlined in Chapter 6.

10.6 Evaluation and Comparison of Improved Nonlinear Static Procedures

The improved procedures were evaluated in an independent study. This study utilized nine EPP oscillators with three different periods and three different strength values. These were subjected to thirteen ground motions for class C sites. The motions were scaled in accordance with the *NEHRP Recommended Provisions for Seismic Regulations for New Buildings and Other Structures* to match a *NEHRP* design-response spectrum. Estimates of maximum displacements were calculated utilizing both current procedures and the proposed improved procedures. This was done using both the NEHRP design spectrum and the average spectrum for the scaled ground motions. This study was not comprehensive enough to make broad general conclusions. However, a number of key observations were made:

- The improved procedures do not exhibit large differences between displacement modification and equivalent linearization approaches. This differs from previous experience with the ATC-40 Capacity-Spectrum Method and the FEMA 356 Coefficient Method.
- The improved procedures also produced more accurate estimates of displacements when compared to response-history analysis results than those produced by the current nonlinear procedures. For displacement ductility of less than ten, the new procedures produced estimates that were within one standard deviation of the response-history results.
- Improved procedures also seem to work well, at least for the case that was studied, in estimating maximum displacement response in conjunction with a design spectrum. Further investigations are warranted to assess the uncertainty involved with this approach on a more general basis.
- The results of the evaluation of the improved nonlinear procedures illustrate the dispersion of results from nonlinear response-history analysis using design level ground motions. This dispersion is the result of the many uncertainties involved in inelastic seismic analysis. It is important for practitioners to keep this in mind when interpreting the results of inelastic analyses.

10.7 Soil-Structure Interaction Effects

There is a perception among many in the practicing engineering community that short, stiff buildings do not respond to seismic shaking as adversely as might be predicted analytically. There are several reasons why short-period structures may not respond as conventional analysis procedures predict. Among these are:

- radiation and material damping in supporting soils;
- structures with basements that experience reduced levels of shaking;
- incoherent input to buildings with relatively large plan dimensions; and
- inaccuracies in modeling, including lumping of masses, neglecting foundation flexibility and some elements that contribute to strength.

These factors are often cited qualitatively, along with the observed good performance of such buildings in past earthquakes, as justification for less onerous seismic demand parameters in codes and analytical procedures. Traditional design procedures have evolved accordingly. Consequently, FEMA 356 currently contains limitations (caps) on the maximum value of the coefficient C_1 for short-period buildings. Many practicing engineers routinely use the limitations on C_1. Capping leads to prediction of maximum inelastic displacements that are less than predicted by the current empirical relationship by a margin that varies widely depending on period, strength, and site conditions. For periods of interest for most buildings (> 0.2 sec. or so), the margin ranges from relatively small (< 20%) for firm (Class B) sites to rather large (> 200%) for soft (Class E) sites.

Chapter 8 presents procedures to incorporate soil-structure interaction (SSI) into nonlinear static analyses. The objective is to replace the subjective limits with rational technical justifications for reducing seismic demand. These SSI techniques address the first three items listed above. The distribution of mass is not addressed in this document; however, it is worthy of future investigation to further improve inelastic analysis procedures.

FEMA 356 and ATC-40 contain similar procedures for incorporating the strength and stiffness of foundations into structural models for inelastic analyses. These procedures result in changes in response compared to fixed base assumptions that can be very significant for some structures. These changes include:

- lengthening of period of the system;
- distribution of forces and displacements among elements;
- sequence of inelastic behavior; and
- potential foundation modes of inelastic behavior (e.g. rocking, soil crushing, pier/pile slip).

Relatively stiff foundation elements on, or in, soil tend to average overall shaking effects to an intensity that is lower than localized maximums. These kinematic effects depend on the plan dimensions of the structure, its embedment into the soil, and its period. They can be visualized as a low-pass frequency (high-pass period) filter on the free-field ground motion. (see Figure 10-3). For nonlinear static procedures this leads to a reduced spectrum representing a foundation input motion. That is, this effect tends to minimize the amplitude of high frequency motion experienced by the structure.

Relative movements in the soil beneath structures dissipate energy through both radiation damping and hysteretic damping. Hysteretic damping is implied in the nonlinear force-deformation properties of the geotechnical components of foundation models, when these elements are modeled. Radiation damping can be incorporated into inelastic analysis procedures by estimating foundation damping and combining it with the conventional assumption for the structure to generate an initial system damping ratio for the system. For NSPs, the result is a further modification in initial spectral ordinates, depending primarily upon the foundation area and effective moment of inertia.

The basic principles used for the development of the SSI procedures in Chapter 8 have been included in the *NEHRP Recommended Provisions for New Buildings* (BSSC, 2000)[1] for the linear analysis and design of new buildings for a number of years. They have been adapted for use with inelastic procedures. They are applicable to both the displacement modification and equivalent linearization forms of nonlinear static analysis.

10.8 Multiple-Degree-of Freedom Effects

Whether evaluating performance or designing a structure, the engineer makes decisions primarily based on component forces and deformations. These are typically compared to some type of acceptability criteria. The intensity of component deformations and

1.Superseded in 2003 with the FEMA 450 *Recommended Provisions for Seismic Regulations for New Buildings and Other Structures.*

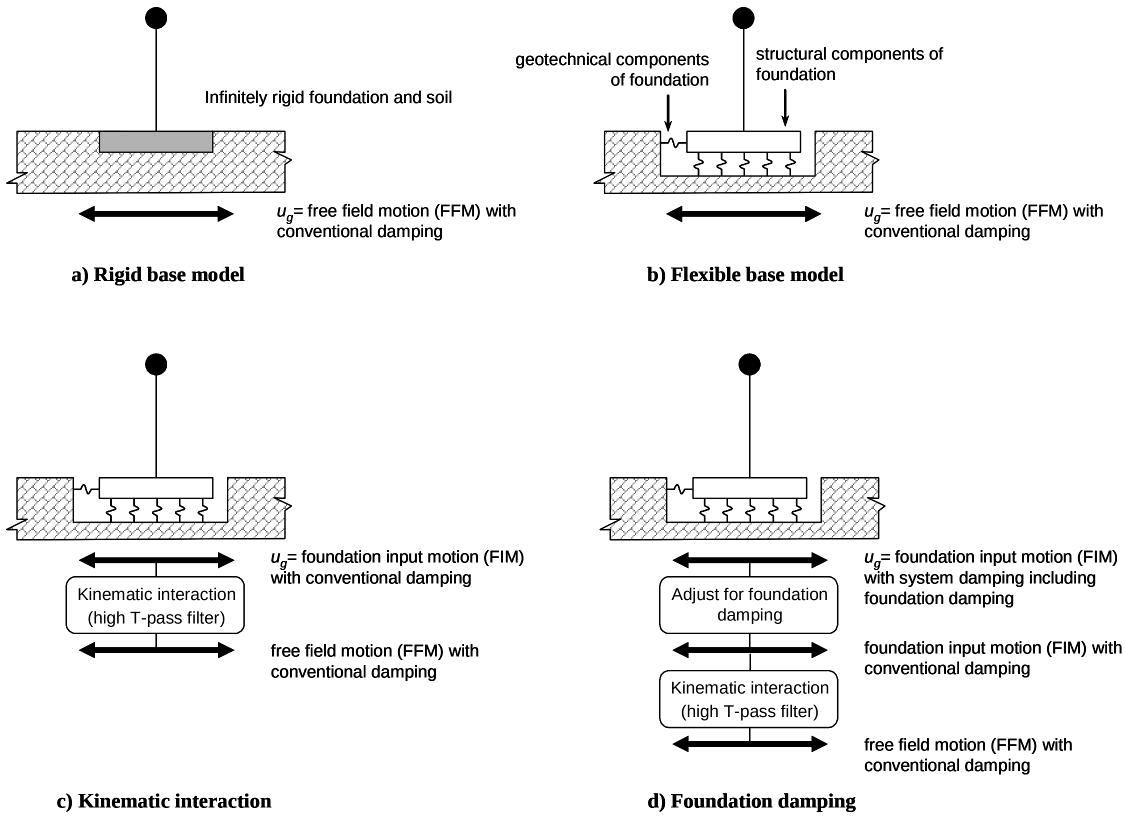

Figure 10-3 Foundation modeling alternatives

forces are directly related to a global displacement parameter (i.e., roof displacement or first-mode spectral displacement) in NSPs. The approximate relative distribution of elastic and inelastic forces and deformations for the multiple-degree-of-freedom (MDOF) structure are controlled by the characteristics of the single-degree-of-freedom (SDOF) model pushover curve assumed in the analysis. The variations of these parameters in a true multi-degree-of-freedom system from those of the SDOF approximation are known as MDOF effects. The adequacy of simplified procedures to address MDOF effects has been questioned by a number of researchers.

Chapter 9 summarizes the options for different load vectors used to generate SDOF pushover curves for structures. In order to investigate and illustrate these various options for evaluating MDOF effects, a comprehensive study of five buildings compared approximate estimates from NSPs for several parameters to those obtained from nonlinear MDOF response-history analyses. The results are consistent with previous research. Practical implications for structures with significant MDOF effects are:

- NSPs generally provide reliable estimates of maximum floor and roof displacements. They also are capable of providing reasonable estimates of the largest inter-story drifts that may occur at any location over the height.
- NSPs are not particularly capable, however, of accurately predicting maximum drifts at each story, particularly within tall flexible structures.
- NSPs are very poor predictors of story forces, including shear forces and overturning moments in taller structures.
- The use of the first-mode load vector is suggested due to the relatively good displacement estimates made with this assumption. Other single-load vectors were less consistent in producing reliable results. The use of two single-load vectors to try to envelope response parameters is not particularly useful.
- Multi-mode pushover analysis consisting of the use of multiple load vectors proportional to the mode shapes of the structure that are statistically combined shows promise in producing better estimates in inter-

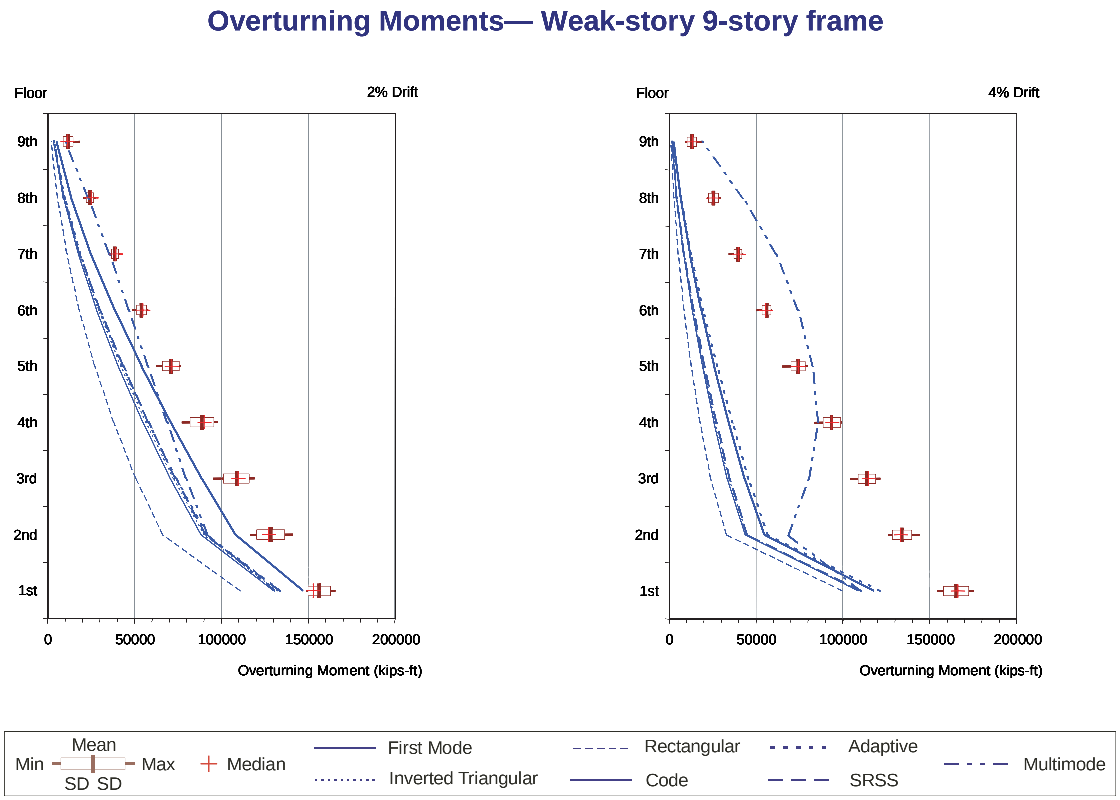

Figure 10-4 Overturning moments in example 9-story building using various load vectors.

story drifts over the heights of the buildings. Current results documented in the literature conclude that the adequacy of results from multi-mode pushover analyses depends on the parameter of interest. It seems that future developments may further improve multi-mode pushover analysis.

- The provisions of FEMA 356 as to when higher modes are to be considered significant are not particularly reliable. All of the example buildings in Chapter 9 would have satisfied the criteria (i.e., higher modes would not have been significant). This is in spite of the fact that all of the buildings, in one way or another, showed sensitivity to higher-mode effects.
- Specific limitations as to when NSPs produce reliable results for MDOF structures are elusive. Chapter 9 provides a discussion of important considerations, but at this time considerable judgment on the part of the practicing engineer is required.
- As a result of the study, it was observed that, in many cases, a single time history response of a multi-degree-of-freedom model gave better indications of drifts and story forces than any of the approximate single-degree-of-freedom estimates (see Figure 10-4). This suggests that a future procedure might be developed that utilizes a small number of response histories to estimate variation and MDOF response parameters.

10.9 Uncertainty and Reliability

NSPs are an important part of performance-based engineering. Performance-based engineering departs from traditional practices in a number of ways. One of the more important departures relates to the treatment of uncertainty and reliability. Uncertainty arises from the seismic ground motion, the structural model, and the analysis technique utilized. Traditional prescriptive analysis and design procedures (e.g., working stress design, load and resistance factor methods) incorporate margins of safety in the calculation of demand and capacity. These procedures treat uncertainty implicitly and they are appropriately conservative with respect to the actual potential consequences. In contrast, performance-based procedures can be used to predict

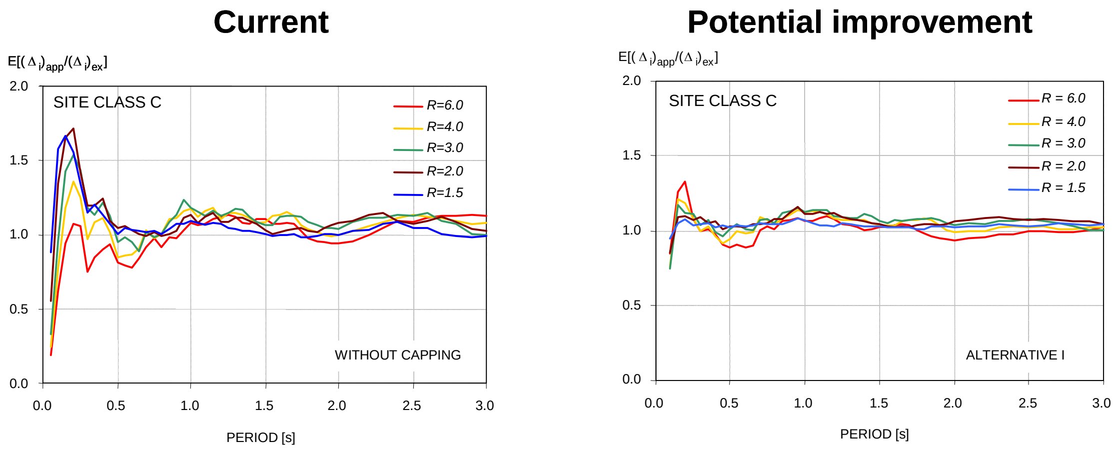

Figure 10-5 Error associated with the Coefficient C_1 as formulated in FEMA 356 (left) and the potential improved formulation (right).

the expected consequences of future ground motions. When used in this manner, the results of the analysis are central (i.e., mean or median) values. This means that they represent the most likely, or "expected," response. However, this also means that the actual response has roughly a 50% chance of being greater and a 50% chance of being less than the predicted response.

The improvements to existing procedures proposed in the document have been developed to optimize predictions of expected values. An example is illustrated in Figure 10-5 showing the error associated with the current FEMA 356 value for coefficient C_1 and a potential improved formulation. The error is determined by dividing the approximate prediction of displacement by the expected value from the response history analyses. The expected value in this case is the mean of results for twenty different ground motion records for each period (T) and for each strength (R). The closer the error is to 1.0, the better the approximate result. Thus the potential improvement clearly provides more accurate results than the current procedure. However, the dispersion of the results for the twenty ground motions is not apparent in this illustration.

The independent evaluation of the proposed improvements is summarized in Chapter 7. In this study, a series of bilinear EPP oscillators with post-elastic stiffness equal to 5% of the initial stiffness were subject to thirteen ground motion records. The results of the nonlinear dynamic (response-history) analyses for an oscillator with a period of 0.5 s are shown in Figure 10-6 for several different strengths. Note the dispersion of the results on either side of the mean (expected) value. Note also that the dispersion increases with lower strength (higher R), as is typical in most cases.

In general, it is important to recognize the empirical nature of the improved expressions for the proposed modifications in this document. They are formulated by attempting to match actual analysis data. They may appear complex, but they do not imply accuracy beyond that associated with the statistical variation in the underlying data. Scrutiny of the detailed characteristics of the data indicates significant uncertainties in expected values. The degree of uncertainty increases for:

a. shorter period;

b. lower strength (higher R);

c. degrading hysteretic behavior; and

d. near-source ground motion.

When applying these procedures, it is important to estimate basic parameters as carefully as possible. For example, using a conservative (low) estimate of the strength of a structure may lead to a conservative (high) estimate of displacement. It is suggested that realistic estimates for all parameters be used to generate expected values as a result of the analysis. Then engineering judgment may be applied to inject the appropriate degree of conservatism, considering the

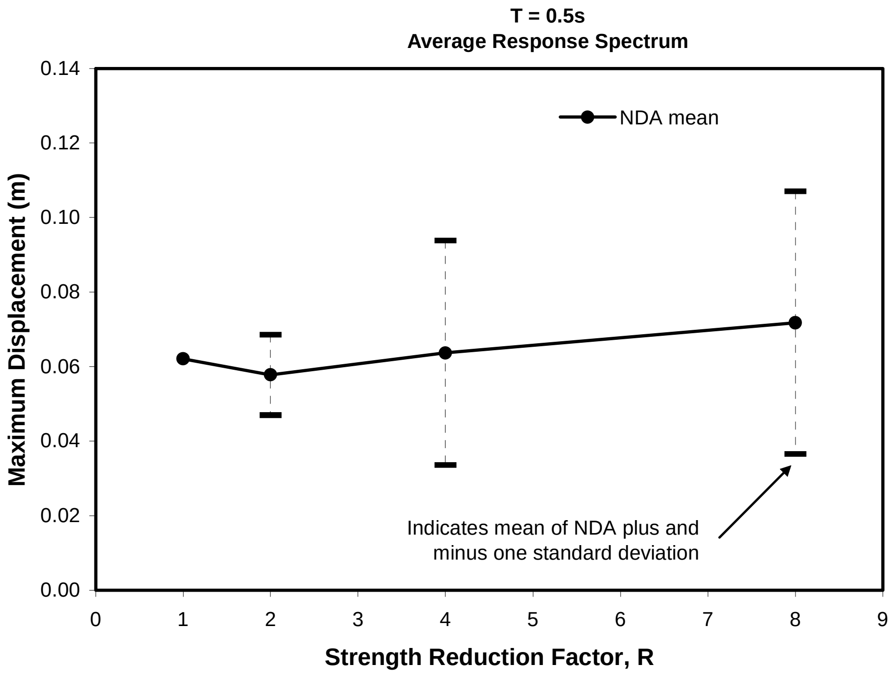

Figure 10-6 Dispersion of results for the nonlinear dynamic analysis (NDA) of a SDOF oscillator subject to thirteen NEHRP Site Class C ground motions

particular circumstances. With this in mind, it should be noted that traditional design equations, including some of those in FEMA 356 and ATC-40, are conservative and may underestimate strength capacities and deformation acceptability for some structures and components. More accurate supplemental information is available from other sources (FEMA 306/307/308, FEMA 355C).

10.10 Important Future Developments

The proposed improvements to nonlinear static analysis procedures in this document will lead to better results in practice. Nonetheless, not all of the shortcomings of NSPs have been addressed. In developing the improvements, a number of important observations about the need for future improvement of inelastic seismic analysis procedures have emerged. These are summarized in the following sections.

10.10.1 Nonlinear Modeling for Cyclic and In-Cycle Degradation of Strength and Stiffness

FEMA 440 makes a distinction between two types of degradation of stiffness and strength of inelastic single degree-of-freedom oscillators (see Figure 10-1). This distinction had not previously been addressed explicitly by guidelines for nonlinear static procedures. Independent studies demonstrate that if strength degradation occurs cyclically, then dynamic response of SDOF systems is stable. In contrast, in-cycle loss of strength can lead to dynamic instability. It is vitally important to be able to differentiate between these two types of structural degradation. Current nonlinear static pushover procedures cannot fully distinguish between cyclic and in-cycle strength degradation. FEMA 440 includes interim recommendations based solely on judgment for this purpose.

Important questions include:

- What current data exist on force-deformation behavior and strength degradation of components subjected to large ductility demands in a single cycle of loading?

- How does in-cycle strength loss in components affect the global dynamic stability of structural models?
- Can this effect be adequately incorporated into NSPs?
- What practical guidance can be provided for the incorporation of in-cycle degradation into nonlinear response-history analysis procedures?
- How can these effects be incorporated into simplified models?

10.10.2 Soil and Foundation Structure Interaction

While some advances are made in FEMA 440, there is not completely adequate guidance for addressing the effects of the interaction between structures and supporting foundations and soils. This is particularly important for short-period or large-footprint structures, where current models may over-predict the input ground motion. Furthermore, additional guidance on force-deformation relationships and damping characteristics of foundations is needed. Finally, there is an important need for adequate guidance on the effect of foundation rocking on structural response.

FEMA 440 supplements existing NSPs with preliminary recommendations for the inclusion of soil-structure-interaction effects (see Figure 10-3). These recommendations augment the existing guidelines in FEMA 356 and ATC-40 for soil-foundation stiffness and strength with approximate procedures to account for kinematic SSI and soil damping. The provisions for soil load-deformation behavior provide a framework primarily with some default values for typical materials. The documents recommend site-specific studies if performance is significantly affected by soil properties.

Important issues include:

- Is the adaptation of linear SSI procedures for nonlinear analysis presented in FEMA 440 adequate as is, or are further adjustments warranted?
- What information is available on soil load-deformation characteristics that might be adopted for general practical application?
- What analytical procedures are available to geotechnical engineers to estimate critical soil properties for inelastic seismic analysis?
- What are the effects of foundation rocking on inelastic seismic response and how can these effects be incorporated into practical analysis procedures?
- What are the effects of foundation sliding on inelastic seismic response and how can these effects be incorporated into practical analysis procedures?

10.10.3 Nonlinear Multi-Degree of Freedom Simplified Modeling

Current nonlinear static procedures are based on single-degree-of-freedom models, which, while simple to understand, are very limited in their ability to address complex structures and multiple-degree-of-freedom effects from input seismic ground motions. As noted, FEMA 440 recognizes that current NSPs are limited in the ability to reliably predict the effects of inelastic behavior of MDOF systems. Specifically, predictions of maximum story drifts, story forces, and inelastic component demands (i.e., plastic hinge rotations) are not reliable using a single-load vector. FEMA 440 also notes that current procedures for using multiple-load vectors representative of the fundamental mode and one or more higher modes (multi-mode pushover analysis) can improve results somewhat, particularly for prediction of maximum story drifts. Ongoing research suggests that multi-mode pushover procedures might be modified to provide better estimates of other demand parameters as well. These improvements come at the expense of greater computational effort and less transparency, however. These barriers have been cited as obstacles to the practical application of nonlinear analysis techniques (i.e., using response-history analysis). This raises the question: why not devote the effort to simplified nonlinear response-history analysis?

One of the interesting observations about MDOF effects during the preparation of the FEMA 440 report was that, in spite of significant dispersion among records, any single nonlinear response-history analysis result often produced better estimates of maximum engineering demand parameters than any of the approximate analyses (see Figure 10-4). This observation suggests that there may be an analysis procedure that characterizes global engineering demand as the maximum displacement response of a structural model subject to shaking hazard represented by currently available regional maps (i.e., by the maps currently prepared by the U.S. Geological Survey for the National Earthquake Hazards Reduction Program). Maximum displacements might be estimated using nonlinear static procedures. Story-level and component-level engineering demand could then be estimated using a simplified MDOF response-history analysis for a small number of ground motion records, scaled to result in the previously estimated global displacement demand. This approach could greatly simplify nonlinear response-history analysis.

Nonlinear response-history analysis might be facilitated further by the use of simplified structural models. Detailed structural models often can require hundreds of degrees of freedom, making the process prone to error and complicating the interpretation of results. As noted in FEMA 440, many practitioners have used innovative sub-structuring techniques to generate "stick" or "fishbone" models that greatly simplify data management, computational effort, and visualization of results.

In summary, this issue presents the following critical questions:

- What are the limits (e.g. periods, separation of modes, mass participation) for building models when MDOF effects must be considered significant?
- Can multi-mode pushover procedures provide adequate results for systems with significant MDOF effects?
- Can maximum engineering demand below the global level (i.e., story and component levels) be predicted using a limited number of nonlinear response-history analyses?
- How should ground motion records be scaled to produce global maximum displacement demands that are representative of a specific shaking hazard?
- How can MDOF structural models be simplified while still providing reliable results for practical application?
- How can strength and stiffness degradation (see Section 10.10.1) be adequately represented in MDOF structural models?
- How can improved methods for modeling foundations and soil structure interaction (see Section 10.10.2) be incorporated into MDOF structural models?
- What is the effect of concentrating masses at story levels on inelastic response, particularly for relative short structures?

10.11 Application Example

This section contains structural analysis calculations, and related commentary, utilizing nonlinear static procedures for the analysis of an example building. The steps in this process are presented in the flowchart in Figure 10-7. On the flowchart, tags have been used to identify pertinent sections of FEMA 440 (this document), and also FEMA 356 and ATC-40. The calculations also include similar tags for ease of reference to these three documents. The example illustrates use of both the displacement modification and the equivalent linearization procedures to estimate the maximum displacement of a building model.

10.11.1 Example Building Description

In order to illustrate the application of NSPs, including the suggested improvements in this document, an example building has been developed. It is depicted and described on calculation Sheet 1. This type of construction is typical for relatively small commercial office and/or retail uses. It is assumed to be located in an area of relatively high seismicity. This example is very simple from an analysis perspective since all of the walls are assumed to be identical and the floor and roof diaphragms are assumed to be rigid. The building is also completely regular and symmetrical. Although some actual buildings might be this simple, it is not always the case and the user should not infer that all structures may be reduced to this level of simplicity.

10.11.2 Basic Ground Motion

The basic ground motion spectrum for the example is illustrated on calculation Sheet 2. The selection of the basic ground motion does not differ from current procedures of FEMA 356, ATC-40 and the 2000 *NEHRP Recommended Provisions for New Buildings*. The same assumptions used for the evaluation study summarized in Chapter 7 are used for the example. Values for short- and 1-second period spectral accelerations at the Maximum Considered Earthquake (MCE) level were assumed for 5% damping and site class C, resulting in values S_S = 1.5g and S_1 = 0.6g. Following the procedures in the *2000 NEHRP Recommended Provisions for New Buildings*, the short- and long-period values were modified for site class C to $S_{XS} = F_a S_S$ and $S_{X1} = F_v S_1$, where F_a = 1.0 and F_v = 1.3. Design-basis ordinates then were obtained as $S_{DS} = 2/3 S_{XS}$ and $S_{D1} = 2/3 S_{X1}$. These values were used with the spectral shape defined in the *NEHRP Recommended Provisions for New Buildings*.

10.11.3 Kinematic Soil-structure Interaction

The next step, also illustrated on Sheet 2, is to modify the initial spectrum to account for kinematic soil-structure interaction in accordance with Chapter 8. Note that the kinematic effect associated with the base-slab averaging is considered, but not the effect related to embedment. This is due to the fact that the building,

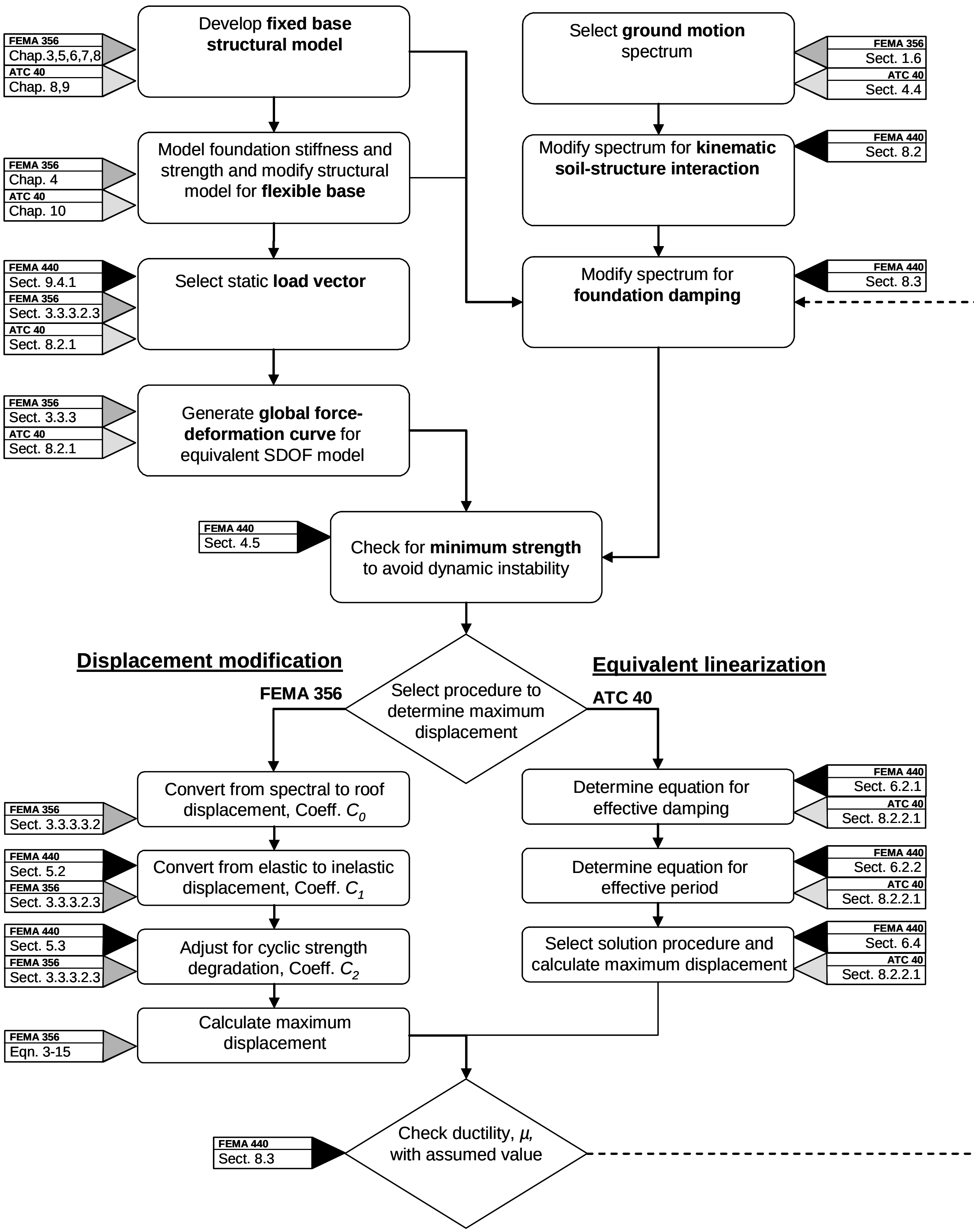

Figure 10-7 Application flowchart for nonlinear static seismic analysis

although supported three feet below grade, does not have a basement. The result of this step is a reduced spectrum representing the foundation input motion.

10.11.4 Fixed-Base Model

The basic procedures to develop a structural model and determine a lateral force and deformation relationship (pushover curve) for a structure remain essentially the same as in ATC-40 and FEMA 356. For the example building, a fixed-based model is relatively simple, as shown on Sheet 3. The fixed-based model is necessary, even if the intention is to include a flexible foundation, due to the fact that foundation damping procedures rely on an estimate of the change in period from a fixed base to a flexible model. The total masses for the building are calculated assuming that the roof weight is approximately 140 psf and that the floors are approximately 160 psf. These estimates are intended to include not only the weight of the structural components of the buildings, but also other dead loads and actual live loads. In an actual application, the weights would be determined in a more detailed take-off. The effective rigidities of the walls are calculated in accordance with the requirements of FEMA 356 and ATC-40 for walls that are cracked. The requirements in this case are identical in both documents.

The linear dynamic properties for the model shown on Sheet 3 are calculated utilizing the basic equations in ATC-40, Section 8.5. In many practical applications, these calculations are done using computer software. The determination of the linear dynamic properties can be simplified by using Rayleigh's method to reduce the number of degrees of freedom in the model to the lateral displacement at the roof and that at the floor level. The process is initiated by estimating a mode shape assuming a uniform acceleration acting on the story masses. Then the deflections at the roof and the floor are calculated. In this case, moment-area calculations were used for this purpose. These displacements are then normalized to a unit displacement at the roof to determine an initial estimate of the fundamental mode shape. Then a first-mode participation factor is calculated. Utilizing the participation factor, modal story forces for unit spectral acceleration can be calculated. This essentially revises the loads that were initially assumed using uniform acceleration. Application of these revised forces to the model results in a change in the displacement at the roof and the floor. These are once again normalized to the roof displacement to generate a revised mode shape. The process continues until the calculated mode shape is essentially equal to that which was assumed. Then the period may be calculated as shown at the end of the calculations on Sheet 3.

10.11.5 Flexible-Base Model

The process continues by repeating the calculations with the assumption of a flexible base, as shown on calculation Sheet 4. The stiffness of the foundation in this case is assumed to be controlled by the soil properties (i.e., foundation structure assumed to be rigid compared to the supporting soil). The initial shear modulus of the soil material is calculated based on the shear wave velocity for the material. For a Class C site, this ranges from 1200 to 2500 feet per second. The effective shear modulus is calculated by reducing the initial value, depending on the severity of shaking at the site. In this case a ratio was determined in accordance with the recommendations of FEMA 356.

Both FEMA 356 and ATC-40 contain equations for calculating rotational and translational stiffness of foundations assuming a rigid plate acting on a homogeneous elastic half space representing the soil. The equations in FEMA 356 differ from those in ATC-40 in their formulation. The equations shown Sheet 4 are from FEMA 356. Essentially the same values can be determined by using the equations in ATC-40. Note that both the rotational stiffness and the translational stiffness are increased due to the embedment of the foundation. It should be noted that the translational stiffness in this case is calculated only for the six shear walls acting in each direction. In reality, the stiffness is probably higher, due to the effect of the foundations beneath the walls acting in the orthogonal direction, as well as the slab on grade that ties all the footings together.

Once the foundation stiffness values are calculated, Rayleigh's method can be used once again to reduce the degrees of translational freedom to two. The calculations to determine dynamic properties for the flexible based model as shown on Sheet 4 are then analogous to those for a fixed base.

10.11.6 Foundation Damping

The next step is to modify the ground motion spectrum further for the effects of foundation damping. The calculations to determine foundation damping are illustrated on calculation Sheet 5. This process begins with an estimate of the effective stiffness of the fixed-base model. Note that the mass must be modified by the effective mass coefficient. The equation for this may be found in ATC-40. The equivalent foundation radius for translation is calculated for the entire footprint of the building. Using this radius, the translational stiffness of the foundation can be estimated using FEMA 440. Note that this estimate corresponds well with that calculated using the actual soil properties on Sheet 4.

The effective height of the building is required to estimate the rotational stiffness of the foundation. This parameter is essentially the centroid of the first-mode shape measured from the base. As noted in Chapter 8, 70% of the total height of the building is often a good approximation. In this example the dynamic properties are used to calculate the actual value. Rotational stiffness of the foundation can then be estimated. Note again that the estimate on Sheet 5 compares reasonably well with that calculated for the flexible-base model using the soil properties of the foundation directly. This leads to an equivalent foundation radius for rotation, which can be visualized as a radius of gyration representing the effective moment of inertia of the foundation.

The actual amount of foundation damping depends on the relative amount of inelasticity in the foundation compared with that in the structure. The procedures in Chapter 8 essentially assume that the inelasticity is concentrated in the structure, which leads to a conservative estimate of foundation damping. The calculation requires an estimate of the system ductility demand. An initial assumption of 3.0 is made for the example. Combining this with an initial damping of 5% leads to an effective damping for the flexible-base model. Combining the foundation damping with the initial assumed damping value (5%) leads to an estimate of the total flexible-base system damping. The foundation input motion calculated, including the effects of kinematic interaction, is based on the initial assumption of 5% damping. The foundation input motion is then modified to reflect the flexible based damping as shown on calculation Sheet 6.

10.11.7 Force-Displacement Relationships (Pushover Curves)

The next step in the process is the selection of a lateral load vector. FEMA 356 and ATC-40 both require and/or suggest a number of options for this selection. Based on the recommendation in Chapter 8, a vector proportional to the first-mode shape is sufficient and preferable to the others; thus the first-mode shape for the flexible-base model is used to generate the basic load-deformation characterizations for the model (see calculation Sheet 7). Two different possibilities are considered. The first case involves an arbitrary assumption that the strength is approximately 0.4 W, resulting in an *R*-factor of 1.52. If the governing inelastic mechanism were foundation rocking or some other ductile mechanism, the pushover curve might be as shown on Sheet 7 for the positive post-elastic stiffness model. Note that a positive post-elastic stiffness of 5% reflects some strain hardening and participation of the slab and columns. If the mechanism included modes of behavior that imply the loss of strength, the post-elastic portion of the curve would have a negative slope for such a degrading system. For the second model, this is assumed to be -25% of the initial oscillator stiffness for the strength-degrading model, as also illustrated in the pushover diagrams on Sheet 7. Each of these cases is examined further.

10.11.8 Check on Minimum Strength for Strength Degrading Model

The model with degrading strength must be checked to determine if there is a potential for dynamic instability, as shown on calculation Sheet 8. The maximum negative post elastic stiffness evident from the pushover curve could be due to cyclic and/or in-cycle loss of strength (including P-Δ effects). As noted in Chapter 4, there is currently no practical means of separating these effects. The suggestion in this document is to assume that the effective post-elastic stiffness, for sites located in the near field, is equal to that attributable to P-Δ effects plus 80% of the balance evident from the pushover curve. For non-near-field sites the percentage drops to 20%. This is strictly a subjective provision and further research is needed on this issue. For the strength-degrading model in the example, dynamic analysis would not be required for the building in either case. However, as noted on Sheet 8, the assumed design level ground motions equal 2/3 of MCE ground motions. Larger motions would imply lower relative strength (higher *R*) for the model. In fact, the MCE motion likely would result in an *R* greater than the maximum allowable and the potential for dynamic instability. This is discussed further below in conjunction with equivalent linearization procedures.

10.11.9 Target Displacement for Displacement Modification

The target displacement for the positive post-elastic stiffness model is calculated using the displacement modification as shown on calculation Sheet 9. The procedure is the Coefficient Method of FEMA 356 modified with the suggested changes for the coefficients C_1 and C_2. The coefficient C_2 is included in the calculation since a concrete structure is likely to have stiffness degradation and pinching hysteretic behavior. Note that the solution for maximum displacement for the strength-degrading model (near- and non-near field) would be the same as the case on Sheet 9, since the displacement-modification procedure does not directly consider negative post-elastic stiffness in the calculation of the coefficients.

10.11.10 Calculation of the Performance Point Using Equivalent Linearization

The solution for the maximum displacement of the positive post-elastic stiffness model using equivalent linearization procedures is shown on calculation Sheets 10 and 11. The effective damping and period calculations for a stiffness-degrading oscillator with positive post-elastic stiffness of 5% are shown on Sheet 10. The selected solution procedure is the construction of the locus of performance points, as shown on Sheet 11. A check using the general equations for effective damping (Equations 6-4, 6-5, and 6-6) and effective period (Equations 6-10, 6-11, and 6-12) produced essentially the same performance point.

10.11.11 Check on Assumed Ductility

The solutions for the positive post elastic-stiffness model are essentially equivalent for displacement modification and equivalent linearization. The resulting ductility demand is approximately 1.8, as opposed to the assumed value of 3.0. This would result in an increase from 6.9% to 7.9% in initial flexible-base damping for the model. This reduces the maximum displacement slightly, but not significantly, in this case.

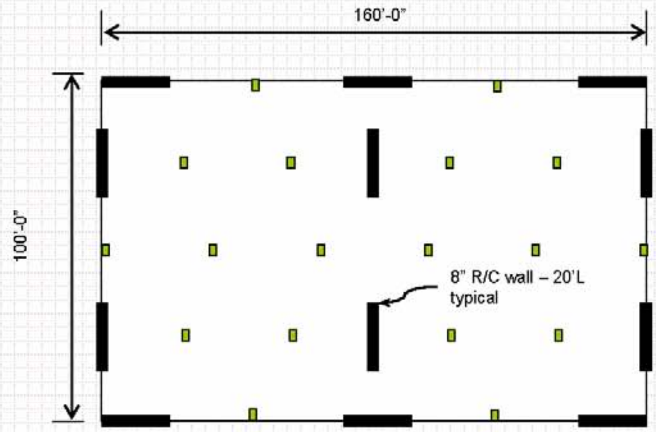

Plan

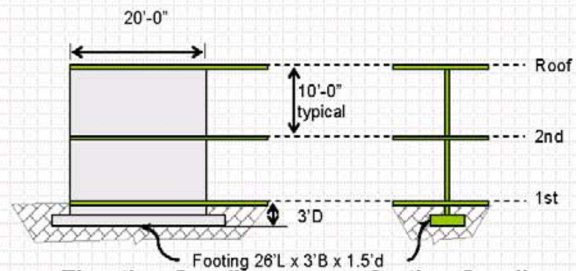

Elevation @ wall

Section @ wall

- **Two story concrete structure:** *FEMA* model buildng Type C2
- **Story to story heights 10 ft:** total building height of 20 ft.
- **Plan dimensions:** 100 ft. by 160 ft.
- **Floors and roof construction:** two-way reinforced concrete flat slab
    - Roof DL = 140 psf
    - Floor DL = 160 psf
- **Vertical support:** concrete columns and interior and exterior reinforced concrete bearing walls
- **Lateral system:** six shear walls in each direction, 12 total – L=20 ft., t=8 in.
- **Foundations:** spread footings bearing 3 ft. below grade and reinforced concrete slab on grade
- **Soils conditions:** very stiff alluvium, v_s = 1200 fps, *NEHRP* Site Class C
- **Ground motion:** shaking with a 10% chance of being exceed in 50 yrs.
- **Analysis objective:** Maximum global displacement for specified ground motion

The analysis procedure is based upon nonlinear static procedures. Both the Coefficient Method of *FEMA 356* and the Capacity Spectrum Method *of ATC 40* are used to estimate the displacement. Both procedures incorporate suggested improvements from *FEMA 440.*

PROJECT:	TITLE:	SHEET:
FEMA 440 **Example Building Analysis**	**Building description**	1

Select ground motion spectrum

FEMA 356 Sect. 1.6
ATC 40 Sect. 4.4

Site class C and shear wave velocity, $v_s = 1200 fps$

Acceleration parameters for MCE shaking

short period $S_s =$ 1.5 g

long period $S_1 =$ 0.6 g

Damping coefficients for initial $\beta = 5\%$

$B_s = 1.0$

$B_1 = 1.0$

Adjustment for site class C

short period $S_{xs} = F_a S_s = (1)1.5 = 1.5g$ $F_a = 1.0$

long period $S_{x1} = F_v S_1 = (1.3)0.6 = 0.78g$ $F_v = 1.3$

To reduce to design level motions (e.g.10% chance of being exceeded in 50 years), multiply accelerations by 2/3

short period $S_{DS} = \frac{2}{3} S_{XS} =$ 1.00 g

long period $S_{D1} = \frac{2}{3} S_{X1} =$ 0.52 g

Modify kinematic soil-structure interaction

Effective foundation size:

a = 100 ft.

b = 160 ft.

$b_e = \sqrt{ab} =$ 126 ft.

Embedment:

e = 0 no basement

$RRS_e = 1.0$

Ratio of response spectra for base slab averaging

$$RRS_{bsa} = 1 - \frac{1}{14100}\left(\frac{b_e}{T}\right)^{1.2} \geq \text{the value for } T = 0.2\text{ sec.}$$

FEMA 440 Eqn. 8-1

Foundation input motion (FIM)

$$(S_a)_{FIM} = RRS_{bsa}\, RRS_e\, (S_a)_{FFM}$$

T	$(S_a)_{FFM}$	RRS_{bsa}	$(S_a)_{FIM}$
0.00	0.52	0.84	0.44
0.10	1.00	0.84	0.84
0.15	1.00	0.84	0.84
0.20	1.00	0.84	0.84
0.30	1.00	0.90	0.90
0.40	1.00	0.93	0.93
0.50	1.00	0.95	0.95
0.60	0.87	0.96	0.83
0.70	0.74	0.96	0.72
0.80	0.65	0.97	0.63
0.90	0.58	0.97	0.56
1.00	0.52	0.98	0.51
1.10	0.47	0.98	0.46
1.20	0.43	0.98	0.43
1.30	0.40	0.98	0.39
1.40	0.37	0.98	0.37
1.50	0.35	0.99	0.34

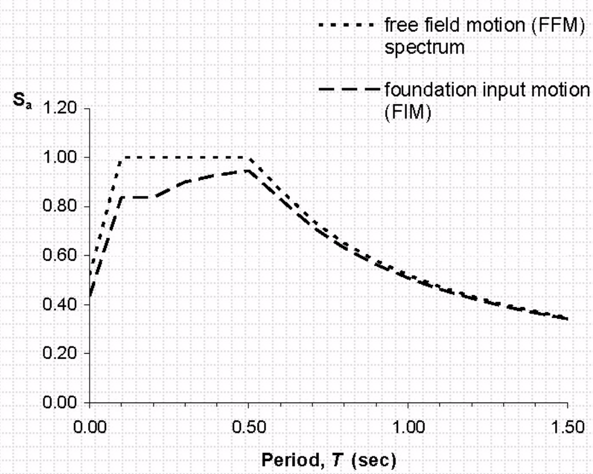

PROJECT:	TITLE:	SHEET:
FEMA 440 Example Building Analysis	**Basic response spectrum and modification for kinematic effects**	2

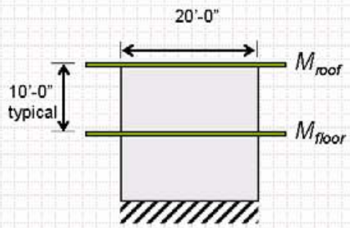

Fixed base model

Total masses

$$M_{roof} = \frac{W_{roof}}{g} = \frac{\text{width(ft.)} \times \text{length(ft.)} \times \text{roof weight(ksf)}}{386.4 \text{ in./sec}^2} = \quad 5.80 \text{ k-sec}^2\text{/in}$$

width= 100 ft
length= 160 ft
roof weight= 0.140 ksf

$$M_{floor} = \frac{W_{floor}}{g} = \frac{\text{width(ft.)} \times \text{length(ft.)} \times \text{floor weight(ksf)}}{386.4 \text{ in./sec}^2} = \quad 6.63 \text{ k-sec}^2\text{/in}$$

width= 100 ft
length= 160 ft
floor weight= 0.160 ksf

Effective rigidities (FEMA 356 Table 6-5; ATC 40 Table 9-3)

Flexural $0.5E_cI_g = 0.5 \times 3{,}000\text{(ksi)} \times \frac{t_w \text{ (in)} \times l_w \text{(in)}^3}{12} \times 6 \text{ walls} =$ 8.3E+10 k-in^2

Shear $0.4E_cA_w = 0.4 \times 3{,}000 \times t_w\text{(in)} \times l_w\text{(in)} \times 6 \text{ walls} =$ 1.38E+07 k

t_w = 8 in $\quad l_w$ = 240 in

Fixed base linear dynamic properties

First-mode load vector (FEMA 440 Sect. 9.4.1)

(estimate with uniform acceleration acting on masses)

F_{roof} = 2240 k $\quad \Delta_{roof}$ = 0.23 in.
F_{floor} = 2560 k $\quad \Delta_{floor}$ = 0.10 in.

Normalize to unit displacement at roof for mode shape $\bar{\phi} = \begin{Bmatrix} \phi_{roof} \\ \phi_{floor} \end{Bmatrix} = \begin{bmatrix} 1.0 \\ 0.4 \end{bmatrix}$

First mode participation factor $PF_m = \left[\frac{\sum_{i=1}^{N} (w_i\phi_{im})/g}{\sum_{i=1}^{N} (w_i\phi_{im}^2)/g} \right] =$ 1.23 (ATC 40 Eqn 8-20)

Modal story forces for unit S_a $F_{im} = PF_m\phi_{im}S_aw_i = \begin{bmatrix} \text{2758 k @ roof} \\ \text{1348 k @ floor} \end{bmatrix}$ (ATC 40 Eqn 8-23)

Displacements due to modal story forces $\delta_{im} = \begin{bmatrix} \text{0.24 in @ roof} \\ \text{0.08 in @ floor} \end{bmatrix}$

Normalize to unit displacement at roof for revised mode shape $\bar{\phi} = \begin{Bmatrix} \phi_{roof} \\ \phi_{floor} \end{Bmatrix} = \begin{bmatrix} 1.0 \\ 0.3 \end{bmatrix}$

Revise modal participation factor

$PF_m = \left[\frac{\sum_{i=1}^{N} (w_i\phi_{im})/g}{\sum_{i=1}^{N} (w_i\phi_{im}^2)/g} \right] =$ 1.22 (ATC 40 Eqn 8-20)

Revise modal story forces for unit S_a $F_{im} = PF_m\phi_{im}S_aw_i = \begin{bmatrix} \text{2744 k @ roof} \\ \text{1038 k @ floor} \end{bmatrix}$ (ATC 40 Eqn 8-23)

Displacements due to modal story forces $\delta_{im} = \begin{bmatrix} \text{0.23 in @ roof} \\ \text{0.07 in @ floor} \end{bmatrix}$

Normalize to unit displacement at roof for revised mode shape (same as assumed) $\bar{\phi} = \begin{Bmatrix} \phi_{roof} \\ \phi_{floor} \end{Bmatrix} = \begin{bmatrix} 1.0 \\ 0.3 \end{bmatrix}$

Period $T = 2\pi\sqrt{\left(\sum w_i\delta_i^2\right) / \left(g\sum F_{im}\delta_{im}\right)} =$ 0.14 sec (ATC 40 Eqn 8-27)

PROJECT:	TITLE:	SHEET:
FEMA 440 Example Building Analysis	**Fixed base structural model**	3

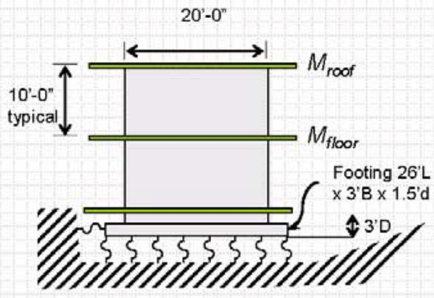

Flexible base model

Soil properties (ATC 40 Sect. 10.4.1.2)

initial shear modulus $G_0 = \frac{\gamma}{g} v_s^2 =$ 31 ksi

unit wt. of soil, $\gamma =$ 100 pcf

shear wave velocity, $v_s =$ 1200 fps

effective shear modulus $G/G_0 =$ 0.75 (FEMA 356 Table 4.7)

$G =$ 23 ksi

Poisson's ratio $\upsilon =$ 0.3

Foundation dimensions

length, L= 26 ft

width, B= 3 ft

thickness, (1.5 ft

depth, D= 3 ft

Rotational stiffness

at surface $K_{\theta,sur} = \frac{GB^3}{1-\upsilon}\left[0.47\left(\frac{L}{B}\right)^{2.4} + 0.034\right] X\ 6walls =$ 780,342,531 k-in/rad (FEMA 356 Fig. 4.4)

embedment factor $\beta_\theta = 1+1.4\left(\frac{d}{L}\right)^{0.6}\left[1.5+3.7\left(\frac{d}{L}\right)^{1.9}\left(\frac{d}{D}\right)^{-0.6}\right] =$ 1.39 (ATC 40 Table 10.2&3)

at depth $K_\theta = K_{\theta,sur}\beta_\theta =$ 1,081,161,315 k-in/rad

Translational stiffness

at surface $K_{x,sur} = \frac{GB}{2-\upsilon}\left[3.4\left(\frac{L}{B}\right)^{0.65} + 1.2\right] X\ 6walls =$ 44,505 k/in (FEMA 356 Fig. 4.4)

embedment factor $\beta_x = \left(1+0.21\sqrt{\frac{D}{B}}\right)\left[1+1.6\left(\frac{Dd(B+L)}{BL^2}\right)^{0.4}\right] =$ 1.86 (ATC 40 Table 10.2&3)

at depth $K_x = K_{x,sur}\beta_x =$ 82,607 k/in

Linear dynamic properties

First-mode load vector (FEMA 440 Sect. 9.4.1)

(estimate with uniform acceleration acting on masses)

$F_{roof} =$ 2240 k $\Delta_{roof} =$ 0.48 in.

$F_{floor} =$ 2560 k $\Delta_{floor} =$ 0.25 in.

Normalize to unit displacement at roof for mode shape $\bar{\phi} = \begin{Bmatrix}\phi_{roof}\\ \phi_{floor}\end{Bmatrix} = \begin{bmatrix}1.0\\ 0.5\end{bmatrix}$

First mode participation factor $PF_m = \left[\frac{\sum_{i=1}^{N}(w_i\phi_{im})/g}{\sum_{i=1}^{N}(w_i\phi_{im}^2)/g}\right] =$ 1.22 (ATC 40 Eqn 8-20)

Modal story forces for unit S_a $F_{im} = PF_m\phi_{im}S_a w_i = \begin{bmatrix}2725 \text{ k @ roof}\\ 1638 \text{ k @ floor}\end{bmatrix}$ (ATC 40 Eqn 8-23)

Displacements due to modal story forces $\delta_{im} = \begin{bmatrix}0.48 \text{ in @ roof}\\ 0.23 \text{ in @ floor}\end{bmatrix}$

Normalize to unit displacement at roof for revised mode shape $\bar{\phi} = \begin{Bmatrix}\phi_{roof}\\ \phi_{floor}\end{Bmatrix} = \begin{bmatrix}1.0\\ 0.5\end{bmatrix}$

(same as assumed)

Period $\tilde{T} = 2\pi\sqrt{\left(\sum w_i\delta_i^2\right)/\left(g\sum F_{im}\delta_{im}\right)} =$ 0.20 sec (ATC 40 Eqn 8-27)

PROJECT:	TITLE:	SHEET:
FEMA 440 Example Building Analysis	**Flexible base structural model**	4

Effective stiffness for fixed base model

$$K^*_{fixed} = M^*\left(\frac{2\pi}{T}\right)^2 = \alpha_m M\left(\frac{2\pi}{T}\right)^2 = \quad 17{,}889 \text{ k/in}$$

FEMA 440 Eqn. 8-3

where

$$\alpha_m = \frac{\left[\sum_{i=1}^{N} w_i\phi_{im}/g\right]^2}{\left[\sum_{i=1}^{N} w_i/g\right]\left[\sum_{i=1}^{N} w_i\phi_{im}^2/g\right]} = \quad 0.77$$

ATC 40 Eqn 8-21

Determine equivalent foundation radius for translation

$$r_x = \sqrt{A_f/\pi} = \quad 71 \text{ ft.} \quad = \quad 856 \text{ in.}$$

FEMA 440 Eqn. 8-4

Determine translational stiffness of the foundation

$$K_x = \frac{8}{2-\upsilon} G r_x = \quad 93{,}867 \text{ k/in}$$

FEMA 440 Eqn. 8-5

Calculate effective building height

$$h^* = \frac{h\sum_{i=1}^{N} M_i\varphi_i}{\sum_{i=1}^{N} M_i} = \quad 174 \text{ in.}$$

FEMA 440 Sect. 8-3

Rotational stiffness of foundation

$$K_\theta = \frac{K^*_{fixed}\left(h^*\right)^2}{\left(\frac{\tilde{T}}{T}\right)^2 - 1 - \frac{K^*_{fixed}}{K_x}} = \quad 6.0\text{E+08 k-in/rad}$$

FEMA 440 Eqn.8-6

Effective foundation radius for rotation

$$r_\theta = \left(\frac{3(1-\upsilon)K_\theta}{8G}\right)^{\frac{1}{3}} = \quad 189 \text{ in}$$

FEMA 440 Eqn. 8-7

Effective period lengthening

Assume $\mu =$ 3

$$\frac{\tilde{T}_{eff}}{T_{eff}} = \left\{1 + \frac{1}{\mu}\left[\left(\frac{\tilde{T}}{T}\right)^2 - 1\right]\right\}^{0.5} = \quad 1.2$$

FEMA 440 Eqn. 8-8

Calculate foundation damping

$$\beta_f = a_1\left(\frac{\tilde{T}_{eff}}{T_{eff}} - 1\right) + a_2\left(\frac{\tilde{T}_{eff}}{T_{eff}} - 1\right)^2 = \quad 3.73 \ \%$$

FEMA 440 Eqn. 8-9a

where

$$a_1 = c_e \exp(4.7 - 1.6h/r_\theta) = \quad 25.19$$

FEMA 440 Eqn. 8-9b

$$a_2 = c_e\left[25\ln(h/r_\theta) - 16\right] = \quad -18.06$$

FEMA 440 Eqn. 8-9c

$$c_e = 1.5(e/r_x) + 1 = \quad 1.00$$

FEMA 440 Eqn 8-9d

Calculate flexible base damping

$$\beta_0 = \beta_f + \frac{\beta_i}{\left(\tilde{T}_{eff}/T_{eff}\right)^3} = \quad 6.9 \ \%$$

FEMA 440 Eqn. 8-10

where $\beta_i =$ 5 %

PROJECT:	TITLE:	SHEET:
FEMA 440 Example Building Analysis	**Determine effect of foundation damping on flexible base damping**	5

Adjust spectrum for flexible base damping

$\beta_0 =$ 6.9 % flexible base damping including effect of foundation damping

$$(S_a)_{\beta_0} = \frac{(S_a)_{5\%}}{B(\beta_0)} = \frac{(S_a)_{FIM}}{B(\beta_0)}$$

FEMA 440 Eqn.6-16

$$B = \frac{4}{(5.6 - \ln \beta_0 (\text{in } \%))} = 1.09$$

FEMA 440 Eqn.6-17

	Free field motion with β=5%		Foundation input motion with β=5%			Foundation input motion with $\beta = \beta_0$	
T	$(S_a)_{FFM}$	$(S_d)_{FFM}$	RRS_{bsa}	$(S_a)_{FIM}$	$(S_d)_{FIM}$	$(S_a)_{\beta}$	$(S_d)_{\beta}$
0.00	0.52	0.00	0.84	0.44	0.00	0.40	0.00
0.10	1.00	0.10	0.84	0.84	0.08	0.77	0.08
0.15	1.00	0.22	0.84	0.84	0.18	0.77	0.17
0.20	1.00	0.39	0.84	0.84	0.33	0.77	0.30
0.30	1.00	0.88	0.90	0.90	0.79	0.83	0.73
0.40	1.00	1.57	0.93	0.93	1.46	0.85	1.34
0.50	1.00	2.45	0.95	0.95	2.32	0.87	2.13
0.60	0.87	3.06	0.96	0.83	2.92	0.76	2.68
0.70	0.74	3.57	0.96	0.72	3.44	0.66	3.16
0.80	0.65	4.08	0.97	0.63	3.95	0.58	3.63
0.90	0.58	4.59	0.97	0.56	4.46	0.52	4.10
1.00	0.52	5.09	0.98	0.51	4.97	0.47	4.57
1.10	0.47	5.60	0.98	0.46	5.49	0.42	5.04
1.20	0.43	6.11	0.98	0.43	6.00	0.39	5.51
1.30	0.40	6.62	0.98	0.39	6.51	0.36	5.98
1.40	0.37	7.13	0.98	0.37	7.02	0.34	6.45
1.50	0.35	7.64	0.99	0.34	7.53	0.31	6.92

Acceleration-displacement response spectra

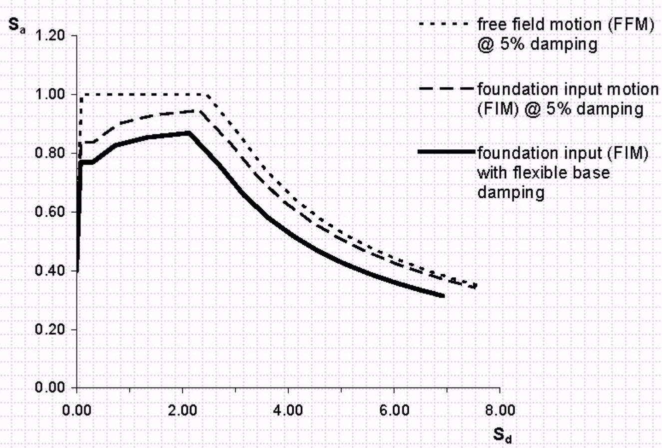

Acceleration vs. period

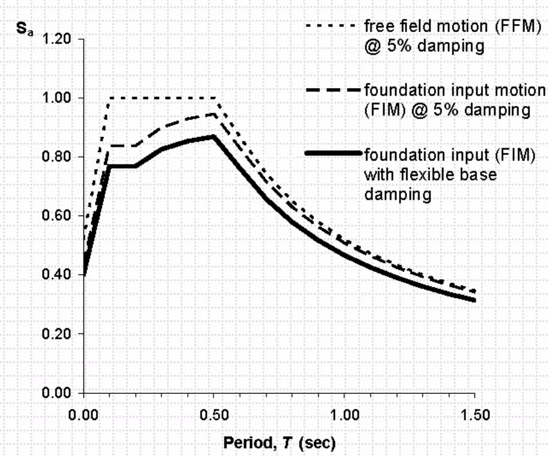

PROJECT:	TITLE:	SHEET:
FEMA 440 **Example Building Analysis**	**Adjust ground motion spectrum for flexible base damping**	6

Non-strength degrading evaluation model

Actual expected base shear strength 0.38 W

Assuming first mode response determine
associated spectral acceleration and associated displacements

Pushover curve

V	Δ_{roof}	
0	0	
0.38	0.23	expected strength
0.48	1.5	a =+5%

ATC 40 Eqn 8-24

$$V_m = \alpha_m S_{am} W$$

$$S_{am} = \frac{V_m}{\alpha_m W} = \quad 0.49 \text{ g}$$

where α_m is the effective mass coefficient for the first mode and
S_{am} is the spectral acceleration that results in a base shear equal to
the expected strength.
Note that α_m is equivalent to C_m in *FEMA 356*.

ATC 40 Eqn 8-26

$$\delta_{im} = PF_m \phi_{im} S_{am} \left(\frac{T_m}{2\pi}\right)^2 g =$$

0.23 in. at roof
0.11 in. at floor

$$R = \frac{S_a}{v_y / W} C_m = \quad 1.56$$

FEMA 356 Eqn 3-16

where PF_m is the first mode participation factor and
ϕ_{im} is the first mode shape.

Strength degrading model

Same strength with post-elastic stiffness= -25%

Pushover curve

V	Δ_{roof}	
0	0	
0.38	0.23	expected strength
0.03	1.10	a = -25%

$$R = \frac{S_a}{v_y / W} C_m = \quad 1.56$$

FEMA 356 Eqn 3-16

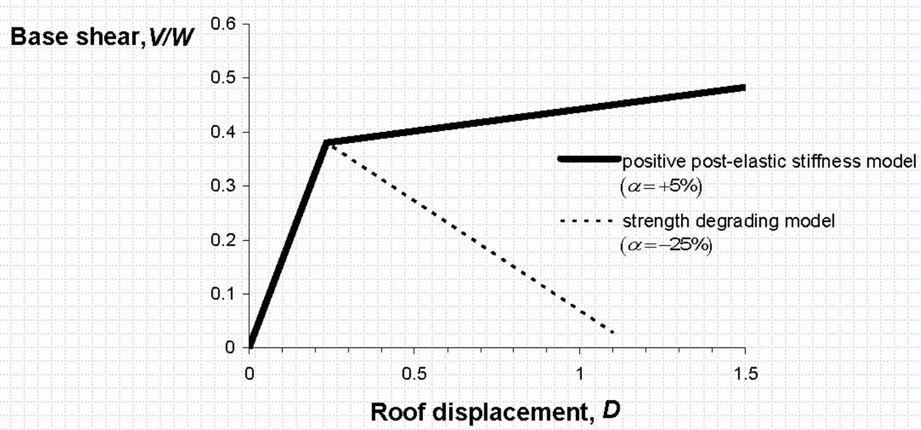

PROJECT:	TITLE:	SHEET:
FEMA 440 Example Building Analysis	**Force-displacement relationships**	7

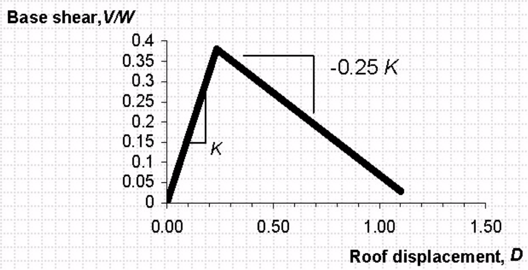

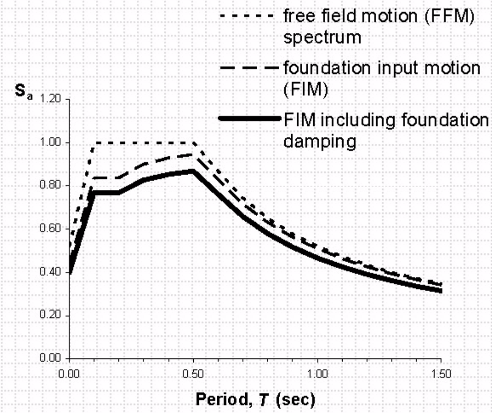

$\alpha_{max} =$ -25%

Strength degrading model

$R = \frac{S_a}{v_y / W} C_m =$ 1.56 — FEMA 356 Eqn 3-16

Check for effective post-elastic stiffness

$\alpha_e = \alpha_{P-\Delta} + \lambda(\alpha_2 - \alpha_{P-\Delta})$ — FEMA 440 Eqn. 4-1

where $\lambda =$ 0.8 near field
0.2 non-near field

assuming that $\alpha_{P-\Delta} \approx 0$ and $\alpha_2 = -25\%$

$\alpha_e =$ -20% near field
-5% non-near field

Check minimum strength

$R_{max} = \frac{\Delta_d}{\Delta_y} + \frac{|\alpha_e|^{-t}}{4}$ — FEMA 440 Eqn. 4-2

where

$t = 1 + 0.15 \ln T =$ 0.76 — FEMA 440 Eqn. 4-3

$R_{max} =$	1.85	near field: greater than	1.56	dynamic analysis not required
	3.42	non-near field: greater than	1.56	dynamic analysis not required

Note: Since the ground motion is for the design 2/3 MCE motion, caution is warranted for possible instability in MCE. This would be particularly critical in the near field.

PROJECT:	TITLE:	SHEET:
FEMA 440 Example Building Analysis	**Check strength degrading model for minimum strength**	8

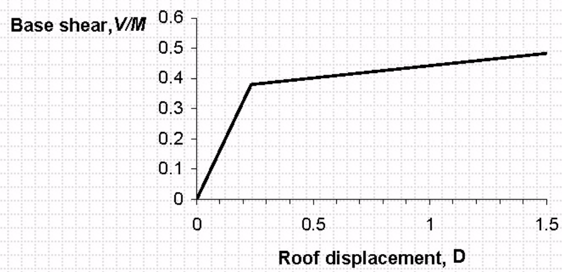

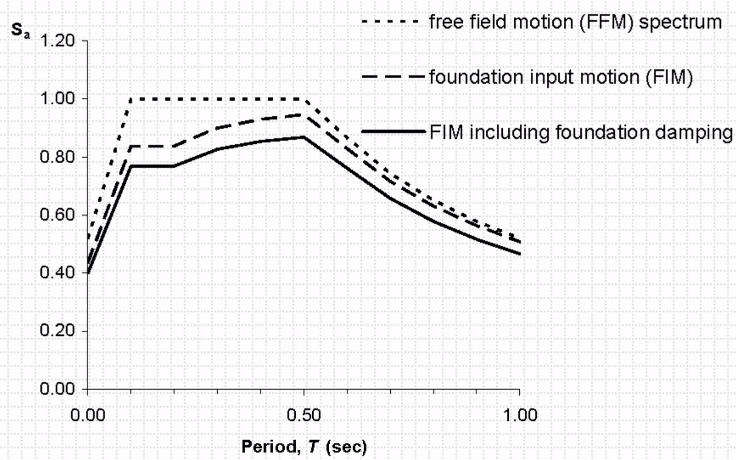

Non-strength degrading evaluation assumption

$$R = \frac{S_a}{V_y / W} C_m = \quad 1.56$$

$$C_0 = \quad 1.22$$

$$C_1 = 1 + \frac{R-1}{aT_e^2} = \quad 1.16$$

FEMA 440 Eqn. 5-1

where a = 90 for Site Class C

$$C_2 = 1 + \frac{1}{800}\left(\frac{R-1}{T_e}\right)^2 = \quad 1.01$$

FEMA 440 Eqn. 5-2

Calulate target displacement

$$\delta_t = C_0 C_1 C_2 S_a \frac{T_e^2}{4\pi^2} g = \quad 0.4 \text{ in.}$$

FEMA 356 Eqn 3-15

PROJECT:	TITLE:	SHEET:
FEMA 440 Example Building Analysis	**Calculate target displacement using displacement modification (*FEMA 356*)**	9

Effective damping

$$\beta_{eff} = A(\mu-1)^2 + B(\mu-1)^3 + \beta_0 \quad \text{For } \mu < 4.0$$

FEMA 440 Eqn. 6-1

$$\beta_{eff} = C + D(\mu-1) + \beta_0 \quad \text{For } 4.0 \le \mu < 6.5$$

FEMA 440 Eqn. 6-2

$$\beta_{eff} = E\left[\frac{F(\mu-1)-1}{\left[F(\mu-1)\right]^2}\right]\left(\frac{T_{eff}}{T_o}\right)^2 + \beta_0 \quad \text{For } \mu \ge 6.5$$

FEMA 440 Eqn. 6-3

Effective period

$$T_{eff} = \left[G(\mu-1)^2 + H(\mu-1)^3 + 1\right]T_o \quad \text{For } \mu < 4.0$$

FEMA 440 Eqn. 6-7

$$T_{eff} = \left[I + J(\mu-1) + 1\right]T_o \quad \text{For } 4.0 \le \mu < 6.5$$

FEMA 440 Eqn. 6-8

$$T_{eff} = \left\{K\left[\sqrt{\frac{(\mu-1)}{1+L[(\mu-2]}} - 1\right] + 1\right\}T_o \quad \text{For } \mu \ge 6.5$$

FEMA 440 Eqn. 6-9

Coefficients for stiffness degrading (STDG) behavior with 5% positive post-elastic stiffness

Damping — FEMA 440 Table 6-1

α(%)	A	B	C	D	E	F
5	5.60	-1.30	10.00	1.80	20.00	0.38

Period — FEMA 440 Table 6-2

α(%)	G	H	I	J	K	L
5	0.18	-0.037	0.15	0.16	0.92	0.05

Effective damping and period as functions of μ

$\beta_0 =$ 7.5 % $\quad T_0 =$ 0.20 sec

μ	β_{eff}	T_{eff}	T_{sec}	M	B
1	7.5	0.20	0.20	1.00	1.12
2	11.8	0.23	0.28	0.69	1.28
3	19.5	0.28	0.33	0.74	1.52
4	22.8	0.32	0.37	0.76	1.62

PROJECT:	TITLE:	SHEET:
FEMA 440 Example Building Analysis	**Calculate performance point using equivalent linearization (*ATC 40*)**	10

Procedure C (MADRS locus of Performance Points)

FEMA 440 Sect. 6.4

Foundation input motion @ 5% damping

MADRS for various μ

			$\mu=1$			$\mu=2$			$\mu=3$			$\mu=4$		
T	$(S_a)_{5\%}$	$(S_d)_{5\%}$	$(S_a)_{\beta_{eff}}$	$(S_d)_{\beta_{eff}}$	MADRS	$(S_a)_{\beta_{eff}}$	$(S_d)_{\beta_{eff}}$	MADRS	$(S_a)_{\beta_{eff}}$	$(S_d)_{\beta_{eff}}$	MADRS	$(S_a)_{\beta_{eff}}$	$(S_d)_{\beta_{eff}}$	MADRS
0.00	0.44	0.00	0.40	0.00	0.40	0.35	0.00	0.24	0.29	0.00	0.22	0.27	0.00	0.21
0.10	0.84	0.08	0.77	0.08	0.77	0.67	0.07	0.46	0.56	0.05	0.41	0.52	0.05	0.40
0.15	0.84	0.18	0.77	0.17	0.77	0.67	0.15	0.46	0.56	0.12	0.41	0.52	0.12	0.40
0.20	0.84	0.33	0.77	0.30	0.77	0.67	0.26	0.46	0.56	0.22	0.41	0.52	0.21	0.40
0.30	0.90	0.79	0.83	0.73	0.83	0.72	0.63	0.49	0.60	0.53	0.45	0.56	0.50	0.43
0.40	0.93	1.46	0.85	1.34	0.85	0.74	1.16	0.51	0.62	0.97	0.46	0.58	0.91	0.44
0.50	0.95	2.32	0.87	2.13	0.87	0.75	1.85	0.52	0.63	1.54	0.47	0.59	1.45	0.45
0.60	0.83	2.92	0.76	2.68	0.76	0.66	2.33	0.45	0.55	1.95	0.41	0.52	1.83	0.39
0.70	0.72	3.44	0.66	3.16	0.66	0.57	2.74	0.39	0.48	2.29	0.35	0.45	2.15	0.34
0.80	0.63	3.95	0.58	3.63	0.58	0.50	3.15	0.34	0.42	2.63	0.31	0.39	2.47	0.30
0.90	0.56	4.46	0.52	4.10	0.52	0.45	3.56	0.31	0.37	2.97	0.28	0.35	2.79	0.27
1.00	0.51	4.97	0.47	4.57	0.47	0.40	3.96	0.28	0.34	3.31	0.25	0.32	3.11	0.24
1.10	0.46	5.49	0.42	5.04	0.42	0.37	4.37	0.25	0.31	3.65	0.23	0.29	3.43	0.22
1.20	0.43	6.00	0.39	5.51	0.39	0.34	4.78	0.23	0.28	3.99	0.21	0.27	3.75	0.20
1.30	0.39	6.51	0.36	5.98	0.36	0.31	5.19	0.21	0.26	4.33	0.19	0.25	4.07	0.19
1.40	0.37	7.02	0.34	6.45	0.34	0.29	5.59	0.20	0.24	4.67	0.18	0.23	4.39	0.17
1.50	0.34	7.53	0.31	6.92	0.31	0.27	6.00	0.19	0.23	5.01	0.17	0.21	4.71	0.16

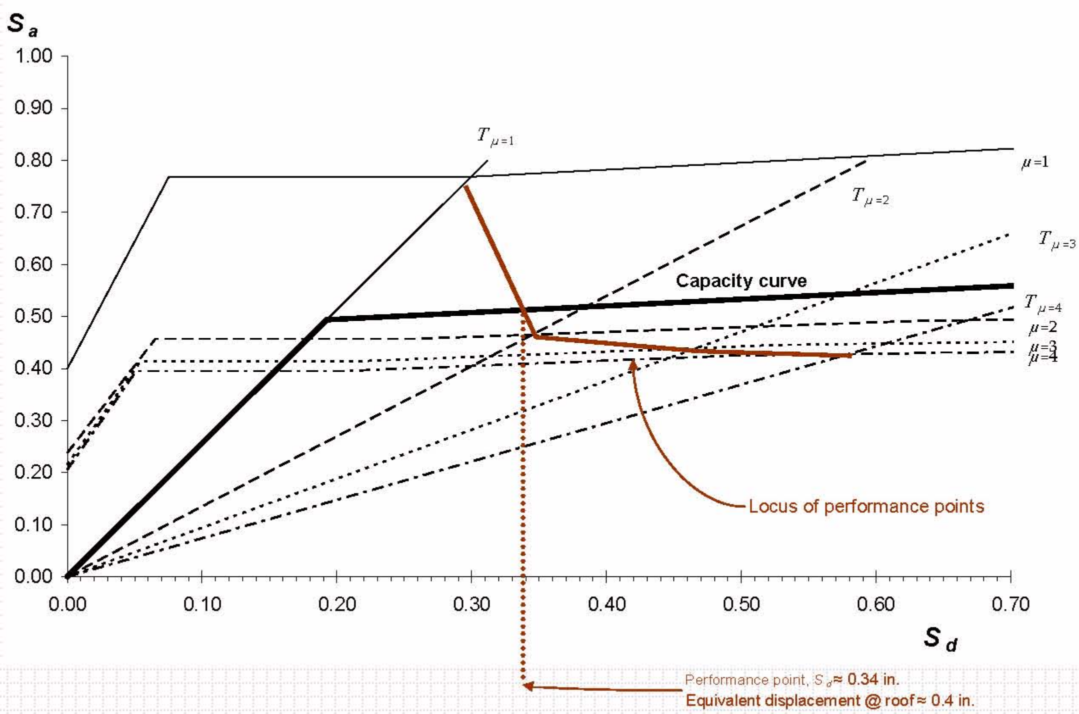

Pushover curve		Convert to ADRS coordinates for Capacity Curve	
V	Δ_{roof}	$S_a = \dfrac{V}{W\alpha}$	$S_d = \dfrac{\Delta_{roof}}{PF}$
0.00	0.00	0.00	0.00
0.38	0.23	0.49	0.19
0.48	1.50	0.98	4.00

PROJECT:	TITLE:	SHEET:
FEMA 440 Example Building Analysis	**Locus of performance points for equivalent linearization**	11

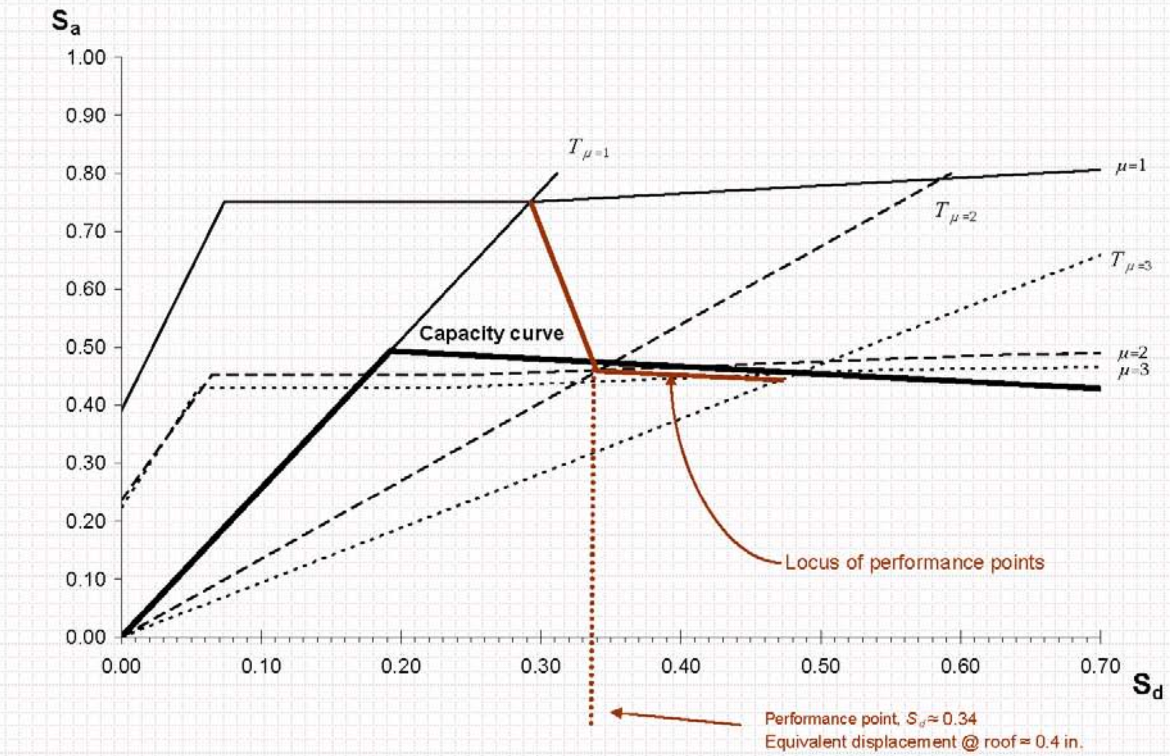

Non-near field case with a_e =- 5%

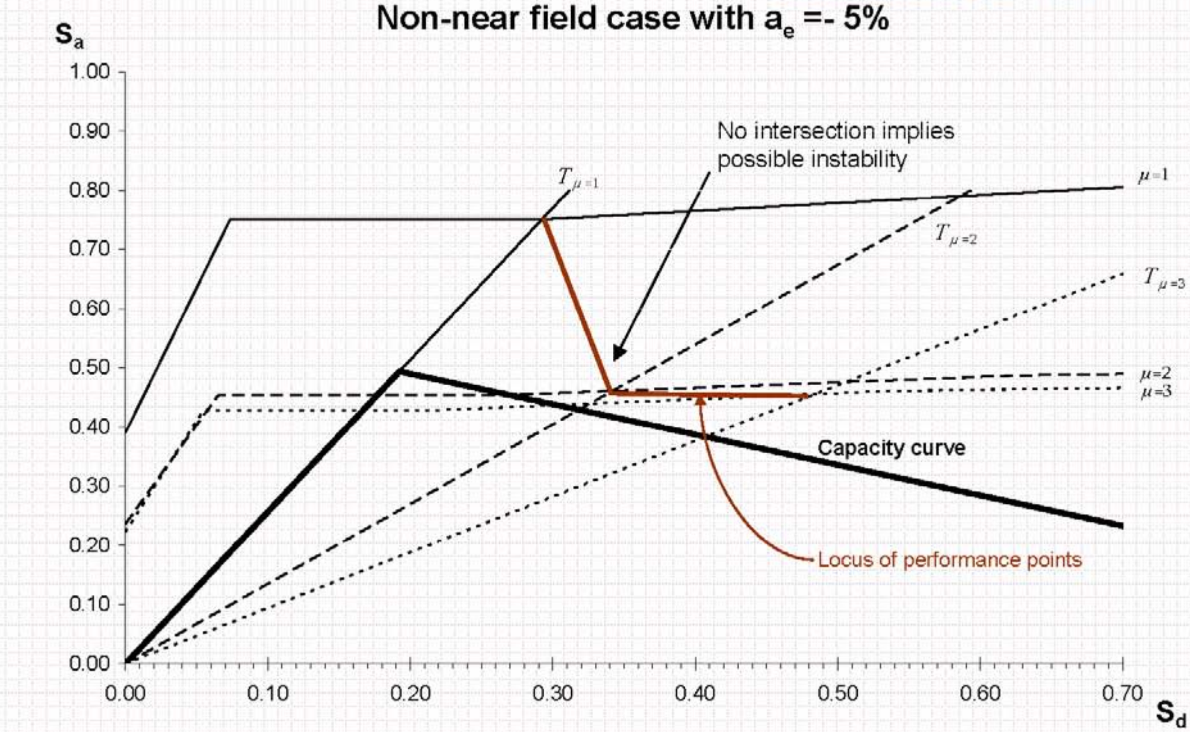

Near field case with a_e=- 20%

PROJECT:	TITLE:	SHEET:
FEMA 440 **Example Building Analysis**	**Equivalent linearization solutions for strength degrading models**	12